AD-A149 294 THEORY AND CALCULATIONS OF THE ELECTRONIC STRUCTURE OF SOLIDS HAVING DIRECTIONAL BONDING(U) MARYLAND UNIV COLLEGE PARK C S WANG APR 83 N00014-79-C-0558 1/1

UNCLASSIFIED F/G 7/4 NL

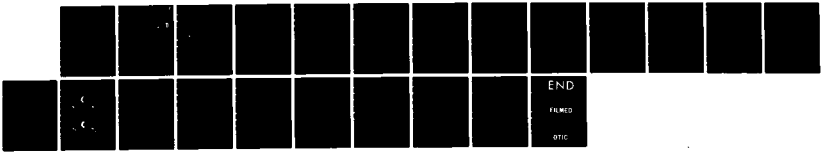

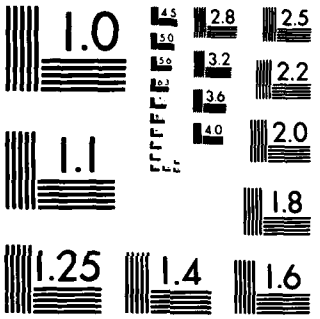

FINAL REPORT
Date April 1983

"Theory and Calculations of the Electronic Structure of Solids Having Directional Bonding"

Progress/Technical Report

ONR Contract #N00014-79-C-0558

by

C. S. Wang

The self-consistent electronic structure of Si, Ge, and zinc-blende GaP, GaAs, ZnS and ZnSe ~~have been~~ were determined using the linear combination of Gaussian orbitals method which ~~has~~ just ~~been~~ developed. A completely general form of the spatial dependence of the potential ~~has been~~ was used to describe accurately the bonding character in the tetrahedral environment. The ground state charge densities we ~~have~~ determined agree very well with experiment (where available) as do the locations of the valence bands, energies, and effective masses. A striking result is that the optical band gaps are underestimated by approximately 30% or more, although the general conduction-band topology is good. This is an inherent difficulty of using the local density approximation for the exchange correlation potential (a theory of the ground state properties) to describe the excitation energies.

The interband optical properties of Si, Ge, GaP, GaAs, ZnS, and ZnSe ~~have~~ were calculated using our self-consistent energies and wave functions. Qualitatively good agreement with experiment is found. Agreement with experiment with regard to line shapes and peak positions

can be improved using an empirical energy dependent self-energy correction as appears in the Sham-Kohn local density theory of excitation. Our results clearly pointed up to the urgent need of an improved theory of the excitation energies in semiconductors and insulators which is being actively pursued under the current contract.

So far, our work has resulted in four extensive manuscripts, one invited paper, and three contributed papers which are enclosed.

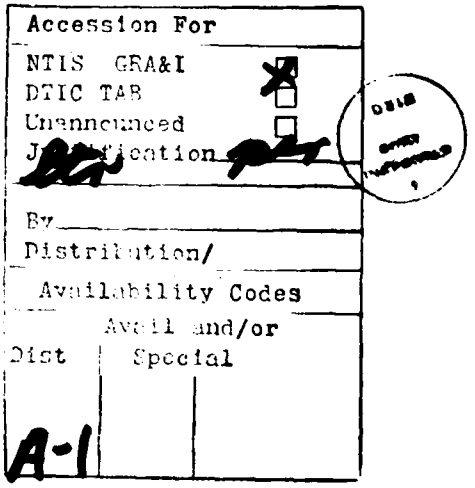

"Develop Theory & Computer Programs"

Progress/Technical Report

ONR Contract # N00014-79-C-0558

by

C. P. Wang

The theory and computer programs have been developed to calculate ab initio energies and wavefunctions of solids where the bonding has important directional characteristics. The self-consistent linear combination of Gaussian orbitals method is used with the exchange and correlation potential included within the local density functional formulism. The crystal potential is expressed as a superposition of spherical Gaussian orbitals centered at each atomic site, plus a Fourier series expansion to accurately describe the bonding character in the tetrahedral environment. The effect of self-consistency on the energy band gaps of diamond and zinc blende semiconductors (e.g. Si and GaAs) is currently under investigation. The application of this method to more complex crystal structures such as Laves phase $ZrZn_2$ (6 atoms/unit cell) is also in progress. Results will be reported shortly at the 1980 APS March meeting.

For the remaining time of the contract major emphasis will be placed on (1) Application of the method to a series of diamond and zinc blende semiconductors in order to make an overall evaluation of the linear combination of Gaussian orbital method, and (2) Develop theory and computational programs necessary to calculate the optical properties and charge densities of these materials in order to make direct comparison of the theoretical energies and wavefunctions with the experimental measurements.

THEORETICAL DETERMINATION OF ELECTRONIC CHARGE DENSITIES IN COVALENTLY BONDED SEMICONDUCTORS

C.S. Wang

University of Maryland
College Park, MD 20742
and
Naval Research Laboratory
Washington, DC 20375

B. M. Klein

Naval Research Laboratory
Washington, DC 20375

Published in Electron Distributions and the Chemical Bond, P. Coppens and M. B. Hall, Editors (Plenum, New York, 1982) p. 133.

THEORETICAL DETERMINATION OF ELECTRONIC CHARGE DENSITIES IN COVALENTLY BONDED SEMICONDUCTORS

C. S. Wang

University of Maryland
College Park, MD 20742
and
Naval Research Laboratory
Washington, D.C. 20375

B. M. Klein

Naval Research Laboratory
Washington, D.C. 20375

INTRODUCTION

In this paper we present theoretical results of electronic charge densities and x-ray structure factors of diamond structure Si and Ge, and zinc-blende structure GaP, GaAs, ZnS and ZnSe. The calculated charge densities result from self-consistent energy band calculations for these crystals using the method of linear combination of Gaussian orbitals (LCGO), with a local density form of exchange-correlation potential. The calculations are fully *ab initio* with the only input being assumed crystal structures and lattice constants. Further details regarding the method may be found in the next section; and the interested reader can find a full discussion and results for the energy bands, densities of states, effective masses and optical properties in Refs. 1 and 2.

Our results discussed in Section III are in good agreement with the experimental structure factor measurements and indicate that local density theory gives a good quantitative representation of the crystal charge density for these, and presumably other materials. This is to be expected as the ground state charge density in local density theory results from a variational principle, with the major uncertainty being the choice of the exchange-correlation functional. It appears that first-principles calculations are capable of yielding results of sufficient accuracy so that reliable interpretations of chemical bonding in materials may be made. Where theory and experiment deviate, principly in the bond density strength and asphericity, improvements may be possible by using more realistic (non-local) exchange-correlation functionals.

METHODOLOGY

An effective one-particle equation for wave vector $\vec{k}$ and band index n can be obtained within the Hohenberg-Kohn-Sham local density functional formalism:

$$\left[-\frac{\hbar^2}{2m}\nabla^2 - \sum_{\mu,\tau}\frac{Z_\tau}{|\vec{r}-\vec{R}_\mu-\vec{r}_\tau|} + \int\frac{\rho(\vec{r}')}{|\vec{r}-\vec{r}'|}d^3r' + V_{xc}(\rho(\vec{r}))\right]\psi_n(\vec{k},\vec{r})$$

$$= E_n(\vec{k})\psi_n(\vec{k},\vec{r}). \tag{1}$$

Here the first term is the kinetic energy, the second the electron-nuclei Coulomb interaction (nuclei charge Z_τ), the third the electron-electron Coulomb potential, and the fourth, the local density exchange-correlation potential. The charge density $\rho(\vec{r})$ is related to the occupied one-particle wave function $\psi_n(\vec{k},\vec{r})$ by

$$\rho(\vec{r}) = \sum_{n\vec{k}}^{\text{occupied}}\psi_n^*(\vec{k},\vec{r})\psi_n(\vec{k},\vec{r}) \tag{2}$$

which in turn determines the electron-electron Coulomb and exchange-correlation potentials. Thus Eqs. (1) and (2) need to be solved self-consistently. We have used the self-consistent linear combination of Gaussian orbitals (LCGO) method[3-5] which has been applied successfully to study the electronic properties of a wide range of simple[6,7] and transition metals,[8-10] and a few covalently bonded materials.[11,12] Here we will give a brief discussion of the procedure that we have adopted to calculate the self-consistent charge density of representative semiconductors.

Linear Combination of Gaussian Orbitals Basis

As in the usual variational treatment, the crystal wave functions $\psi_n(\vec{k},\vec{r})$ are expanded in terms of a Bloch basis set $\phi_{i\tau}(\vec{k},\vec{r})$

$$\psi_n(\vec{k},\vec{r}) = \sum_{i,\tau}C_{i\tau,n}(\vec{k})\phi_{i\tau}(\vec{k},\vec{r}) \tag{3}$$

where the standard LCAO form was used for the basis function i centered at the sublattice site τ,

$$\phi_{i\tau}(\vec{k},\vec{r}) = \frac{1}{\sqrt{N}}\sum_{\vec{R}_\mu}e^{i\vec{k}\cdot\vec{R}_\mu}u_{i\tau}(\vec{r}-\vec{R}_\mu-\vec{r}_\tau). \tag{4}$$

An optimum choice of a basis set $[u_{i\tau}(\vec{r})]$ which provides maximum variational freedom yet still maintains a manageable size of the secular equation has been the subject of numerous discussions.[13] In our study for covalently bonded diamond and zinc-blende materials we have chosen a linear combination of atomic orbitals *minimum* basis set with an additional shell of s, p, and d virtual Gaussian type orbitals (GTO) for added variational flexibility. The atomic orbitals were solutions to the atomic secular equation constructed with the self-consistent Herman-Skillman atomic potential[14] and a basis set of GTO. The Gaussian exponents were varied non-linearly to minimize the atomic energies as follows: For each orbital quantum number we choose a set of even-tempered Gaussians that satisfy

$$\alpha_i = \alpha_1\left(\frac{\alpha_2}{\alpha_1}\right)^{i-1}, \tag{5}$$

where the two most localized Gaussian exponents α_1 and α_2 were varied non-linearly to minimize the corresponding lowest state atomic energy. Typically 8, 5, and 4 GTO were used to describe the atomic 1s, 2p and 3d states, respectively. Two more extended GTO were added with their exponents varied to minimize the energies of the next lowest states. This procedure was continued until all valence states of the atom are completed. The atomic orbitals were then augmented by an additional *s*, *p*, and *d* shell of independent GTO for the variational freedom needed to describe the wave functions in a solid. The presence of these diffuse GTO often leads to approximate linear dependence of the basis set, hence the overlap matrices must be checked carefully against negative or unphysically small eigenvalues throughout the Brillouin zone. We found it helpful to truncate the tail of the highest valence atomic orbitals by setting minimum values for the corresponding Gaussian exponents. Variationally this has little effect because the long tails of the atomic orbitals are strongly modified in a solid by the overlap of the wave functions on the neighboring atomic sites. These changes can only be fitted with the aid of the additional virtual orbitals. The resulting basis set is not complete, but does overlap both the bound and low excited subspaces of the wave functions. It leads to a dimension of 36 × 36 for the secular equation for Si, 45 × 45 for GaP and ZnS, and 54× 54 for Ge, GaAs, and ZnSe.

Crystal Potential

The initial Coulomb potential is constructed as a superposition of overlapping spherically symmetric atomic potentials. The corresponding overlapping atomic charge density is used to evaluate the local density exchange-correlation potential which we chose to be a Wigner interpolation formula[15] of the form (energies are in *Ry*):

$$V_{xc}(\vec{r}) = -2(3/\pi)^{1/3}\rho^{1/3}\left\{1.0 + \frac{(0.0569\,\rho^{1/3} + 0.0060)}{(\rho^{1/3} + 0.079)^2}\right\}, \tag{6}$$

where the charge density ρ is evaluated at the point $\vec{r}$.

Due to the analytic properties of the Gaussian orbitals it is customary to expand the crystal potential in a set of either (1) symmetrized plane waves (SPW)

$$V(\vec{r}) = \sum_s V_s \sum_{\{R|\vec{d}_R\}} e^{iR\vec{K}_s\cdot(\vec{r}-\vec{d}_R)}, \tag{7}$$

where the sum runs over all group operations $\{R|\vec{d}_R\}$ and stars of reciprocal lattice vectors $\vec{K}_s$; or (2) overlapping GTO,

$$V(\vec{r}) = \sum_{\tau,i,\mu} V_{i,\tau}\, e^{-i\alpha_i|(\vec{r}-\vec{R}_\mu-\vec{r}_\tau)|^2} \tag{8}$$

centered at each atomic site.

The plane wave basis has the advantage of being completely general, but the disadvantage of slowly converging near the nuclei due to the Coulomb singularity. For example, even with the aid of an Ewald type procedure, it is necessary to include 4000 stars of reciprocal lattice vectors to describe the crystal potential for Ni[8] and Fe.[9] For a more complex structure with less symmetry, such a procedure can be prohibitively expensive. The GTO on the other hand, converge rather quickly (less than 20 GTO are needed to describe an atomic potential to good accuracy). However, overlapping

spherical GTO are too spherical around each atom to describe the directional bond in a covalent material. Although results can be improved by including higher angular momentum terms around each atom and/or additional GTO centered at the interstitial tetrahedral sites, such a procedure is somewhat arbitrary compared to the Fourier series expansion where the reciprocal lattice vectors are rigorously defined. Thus we chose to expand our potential in a mixed basis of GTO and SPW as proposed by Euwema.[16] The self-consistent Herman-Skillman neutral atomic Coulomb and exchange-correlation potentials were each fitted with 18 even-tempered GTO. The four longest range GTO which can be represented by rapidly converging Fourier series were deleted to avoid excessive lattice sums in constructing the overlapping crystal potential. The difference between the exact atomic Coulomb potential and the truncated GTO series was tabulated over a logarithmic radial mesh and their Fourier coefficients calculated numerically. In general the crystal $V_{xc}(\vec{r})$ cannot be expressed as a superposition of atomic $V_{xc}(\vec{r})$. However, subtracting out the contribution from the overlaping atomic GTO series helps to eliminate the cusp behavior near the nuclei to yield a rapidly converging Fourier expansion for the remainder. Typically 25 independent Fourier coefficients were evaluated via a three dimensional least-square fitting procedure based on a sampling of 400 random points in the unit cell. Having defined the initial potential and the basis functions, it is straightforward to evaluate the usual linear variational secular equation:

$$\sum_{j\sigma} [H_{i\tau,j\sigma}(\vec{k}) - S_{i\tau,j\sigma}(\vec{k}) E_n(\vec{k})] C_{j\sigma,n}(\vec{k}) = 0. \tag{9}$$

When expanded in terms of the basis orbitals $u_{i\tau}(\vec{r})$, the Hamiltonian and overlap matrix elements are

$$H_{i\tau,j\sigma}(\vec{k}) = \sum_{\vec{R}_\mu} e^{-i\vec{k}\cdot\vec{R}_\mu} < u_{i\tau}(\vec{r} - \vec{R}_\mu - \vec{r}_\tau) | \hat{H} | u_{j\sigma}(\vec{r} - \vec{r}_\sigma) > \tag{10}$$

$$S_{i\tau,j\sigma}(\vec{k}) = \sum_{\vec{R}_\mu} e^{-i\vec{k}\cdot\vec{R}_\mu} < u_{i\tau}(\vec{r} - \vec{R}_\mu - \vec{r}_\tau) | u_{j\sigma}(\vec{r} - \vec{r}_\sigma) >. \tag{11}$$

The above two-and three-center integrals for a Gaussian type basis can be expressed in closed form. Results have been published elsewhere.[5,17] The secular equation was solved at a set of $\vec{k}$ points in Brillouin zone and a new charge density was calculated from Eq. (2).

Self-consistency

The major modification to the charge density due to self-consistency (charge transfer, change in valence electron s and p occupation, etc.) are expected to occur in the interstitial region, particularly along the tetrahedral bond. Therefore the Gaussian expansion describing the atomic potential near the nucleus was kept frozen at their starting values; only the Fourier coefficients were varied following the procedure of Callaway and Fry.[18] At each iteration, the Fourier coefficients of the input Coulomb potential $V_c(\vec{K}_s)$ were evaluated from the output charge density $\rho(\vec{K})$ of the previous iteration, with

$$V_c(\vec{K}_s) = \frac{8\pi}{K_s^2} \rho(\vec{K}_s) \tag{12}$$

and $\rho(\vec{K}_s)$ calculated analytically from the wave functions:

$$\rho(\vec{K}_s) = \sum_{n\vec{k}} C^*_{i\tau,n}(\vec{k}) C_{j\sigma,n}(\vec{k}) S_{i\tau,j\sigma}(\vec{k}, -\vec{K}_s). \tag{13}$$

Here the sum runs over all occupied bands (index n) and wave vectors $\vec{k}$, $C_{i\tau,n}(\vec{k})$are the eigenvectors, and the generalized overlap matrices

$$S_{i\tau,j\sigma}(\vec{k}, \vec{K}_s) = \int \phi^*_{i\tau}(\vec{k}, \vec{r}) e^{i\vec{K}_s \cdot \vec{r}} \phi_{j\sigma}(\vec{k}, \vec{r}) d^3r \tag{14}$$

are simply the matrix elements of the plane waves calculated between the basis functions $\phi_{i\tau}(\vec{k}, \vec{r})$. Ten special $\vec{k}$-points[19] in the 1/48'th of the irreducible Brillouin zone were used in our iterations for a self-consistent potential. In order to speed up the convergence, $\rho(\vec{K}_s)$ was relaxed by mixing with 50% of the input $\rho(\vec{K}_s)$ from the previous iteration before it was substituted into Eq. (2). Once $\rho(\vec{K}_s)$ has been determined it is straightforward to calculate $\rho(\vec{r})$ and hence the exchange-correlation potential at the selected points in the unit cell. The contribution from the overlapping GTO are subtracted-out before the new Fourier coefficients $V_{xc}(\vec{K}_s)$ are determined by a 3-dimensional least-square fitting procedure. Finally the plane wave contributions of both the Coulomb and the exchange-correlation potential to the new Hamiltonian were calculated via

$$H_{i\tau,j\sigma}(\vec{k}) = \sum_{\vec{K}_s} (V_c(\vec{K}_s) + V_{xc}(\vec{K}_s)) S_{i\tau,j\sigma}(\vec{k}, \vec{K}_s), \tag{15}$$

where $S_{i\tau,j\sigma}(\vec{k}, \vec{K}_s)$, which needs to be calculated only once, is the same matrix used in Eq. (13) to evaluate $\rho(\vec{K}_s)$. We found that $\rho(\vec{K}_s)$ converges to within 10^{-4} a.u., and the energies to 0.02 eV, at the end of 5 iterations.

In the following section we compare our self-consistent $\rho(\vec{K}_s)$ (Eq. (13)) with experimentally measured structure factors. The *valence* electron charge density maps also shown were calculated with a mixed basis of GTO and SPW. The GTO were obtained by fitting the atomic valence electron charge density $\rho(\vec{r})$, while the effect of self-consistency was included through Eq. (13). The sum over bands was limited to the valence electrons only. Deformation densities, $\delta\rho(\vec{r})$, were calculated by subtracting a superposition of spherical neutral-atom valence densities used as starting values in our SC calculations from the final SC valence charge densities.

RESULTS AND DISCUSSION

In this section we present our results for the valence and deformation charge densities, and the x-ray structure factors calculated according to the procedures described in the preceding section. All of the experimental structure factors used for comparison were reduced to zero temperature and corrected for anomalous dispersion in order to facilitate a meaningful correlation between theory and experiment.

Si and Ge

In Figs. 1-3 we show our calculated valence and deformation density maps and bond axis densities, respectively, for Si and Ge. Tables I and II compares our calculated structure factors, F(*hkl*), with experiment and other *ab initio* theoretical results.

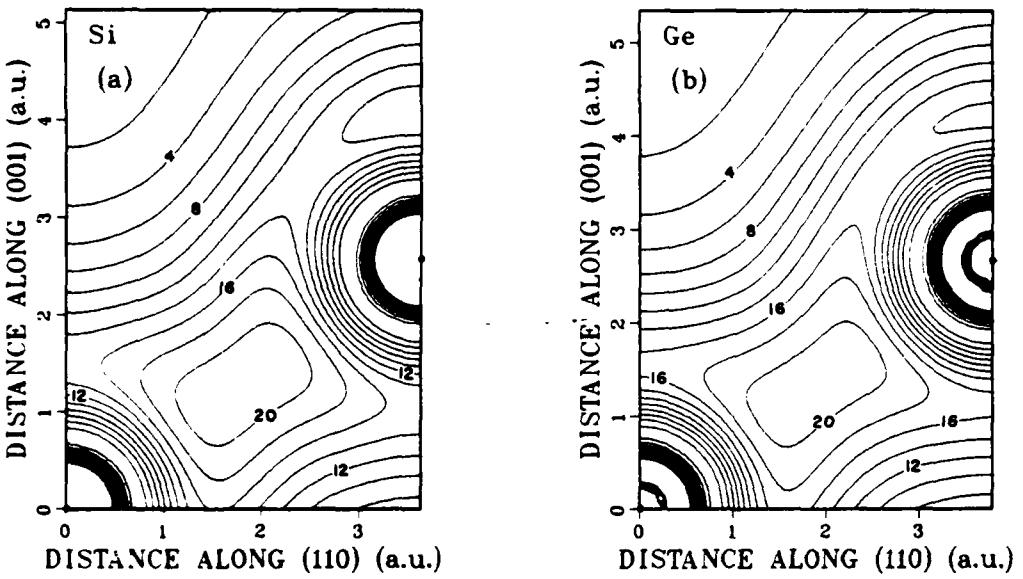

Fig. 1. Calculated self-consistent valence charge density in a portion of the $(1\bar{1}0)$ crystal plane for: a) Si, and b) Ge. The contours are in units of electrons/unit cell, and the contour interval is 2 electrons/unit cell.

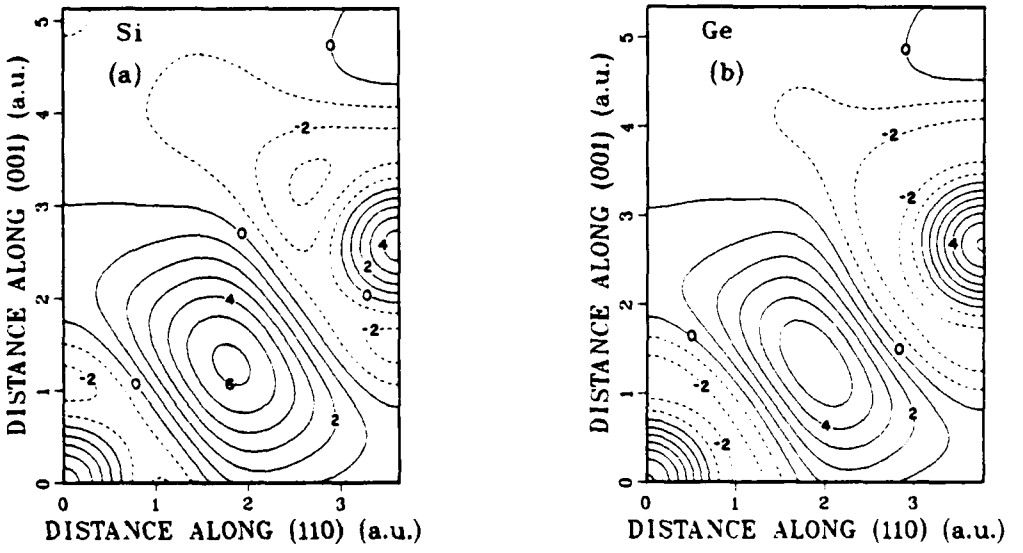

Fig. 2. Calculated valence deformation charge density in a portion of the $(1\bar{1}0)$ crystal plane for: a) Si, and b) Ge. The contours are in units of electrons/unit cell, and the contour intervals is 1 electron/unit cell.

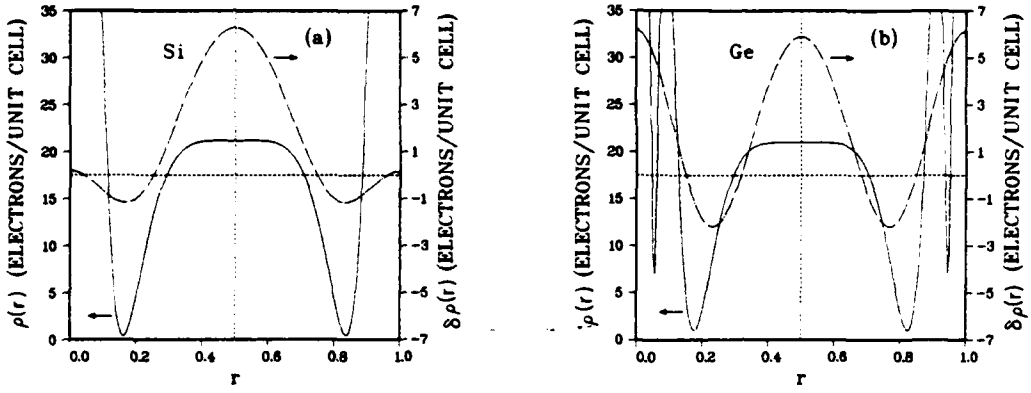

Fig. 3. Calculated $\rho(r)$ (solid lines) and $\delta\rho(r)$ (chain-dotted lines) along the (111) bonding direction for: a) Si, and b) Ge. $\rho(r)$ is the self-consistent valence charge density, $\delta\rho(r)$ is the valence deformation charge density (self-consistent minus starting overlapping atomic charge densities), and r is the fraction of the nearest neighbor (bond) distance.

Table I. Comparison of Theoretical and Experimental X-ray Structure Factors $F(hkl)$ for Si (in Units of Electrons/Unit Cell)

hkl	Expt.[a]	Present Results	Theory[b]	Theory[c]	Theory[d]
000	(28.0)	(28.0)	(28.0)	(28.0)	(28.0)
111	15.19	15.11	15.07	15.12	15.13
220	17.30	17.26	17.31	17.28	17.14
311	11.35	11.37	11.41	11.33	11.02
222	0.38	0.25	—	0.34	0.38
400	14.89	14.92	14.92	14.88	14.70
331	10.25	10.17	10.15	10.20	9.94
422	13.42	13.37	13.37	13.36	13.30
333	9.09	9.07	9.07	9.02	8.92
511	9.11	9.08	9.08	9.08	8.98
440	12.08	12.04	—	12.04	12.00

[a]Experiment: Aldred and Hart, Ref. 27., except for (222) which is from Ref. 28.
[b]LCAO theory: Heaton and Lafon, Ref. 12.
[c]SCOPW theory: Raccah, *et al.*, Ref. 29.
[d]Pseudopotential theory: Zunger and Cohen, Ref. 21.

Table II. Comparison of Theoretical and Experimental X-ray Structure Factors $F(hkl)$ for Ge (in Units of Electrons/Unit Cell)

hkl	Expt.[a]	Present Results	SCOPW[b]
000	(62.0)	(62.0)	(62.0)
111	39.42	38.83	38.95
220	47.44	47.23	47.26
311	31.37	31.29	31.21
222	0.26	0.22	0.48
400	40.50	40.56	40.54
331	27.72	27.39	27.53
422	36.10	35.91	36.00
333	24.50	24.35	24.34
511	—	24.35	24.38
440	32.34	32.23	32.23

[a]Matsushita and Kohra, Ref. 24.
[b]Raccah, *et al.*, Ref. 29.

Figures 1-3 clearly show the covalent nature of the bonding in Si and Ge, with the characteristic charge pile-up near the bond center for both materials. It is further interesting to note from the deformation densities shown in Figs. 2 and 3 how charge is pulled into the bond compared with the situation for overlapping charge densities—much of the covalency results from charge redistribution, not merely from wave function overlap.

The valence and deformation maps are in good agreement with previous *ab initio* calculations[20,12] and the experimental densities constructed by Yang and Coppens[22] for Si. The characteristic features of the valence density being elongated along the bond, and opposite for the deformation density, are reproduced in the calculated maps. However, Yang and Coppens[22] find a valence bond maximum of 27.6, while we find 21.3 (electrons/unit cell) for Si. Our value is very close to the theoretical value found by Hamann[20] (22.2 electrons/unit cell) but somewhat smaller than that found by Zunger and Cohen[21] (24.0 electrons/unit cell). Recently, Scheringer[23] has pointed out that the Yang and Coppens[22] value may be overestimated by as much as 3.6 electrons/unit cell due to inaccuracies in four of the measured high momentum structure factors. For Ge, where experimental structure factor data exists for only a relatively few number of reflections[24,25] ($\sin\theta/\lambda < 0.50\ A^{-1}$), quantitative results for the bonding have been limited.[26]

Calculated and measured structure factors for Si and Ge are compared in Tables I and II, respectively. For silicon, except for the (222) forbidden reflection, the experimental results of Aldred and Hart[27] who used the Pendellösung fringe method are shown in Table I. For the (222) reflection in Si the value shown was chosen from the work of Roberto, Batterman and Keating,[28] corrected to zero temperature (see Ref. 28). The experimental results of Matsushita and Kohra[24] for Ge were chosen for comparison in Table II. These measurements were made using the half-width of the Bragg-case diffraction curves measured in the triple crystal arrangement using Cu-Kα

radiation. Tables I and II also show the present theoretical structure factor results, together with calculated values of: Heaton and Lafon[12] (for Si) who used a self-consistent LCAO method similar to ours but with a Kohn-Sham ($\alpha = 2/3$) exchange-correlation potential and a smaller basis set; Raccah, *et al.*[29] (for Si and Ge) who used a self-consistent orthogonalized plane wave (SCOPW) approach also with $\alpha = 2/3$; and Zunger and Cohen[21] (for Si) who used the first-principles self-consistent pseudopotential method with the Hedin-Lundqvist[30] form of local density exchange-correlation potential.

Our structure factor results for Si compare extremely well with the measurements of Aldred and Hart.[27] Most of the theoretical results also agree very well, especially the present results and the other SC-LCAO[12] and the SCOPW[29] calculations. There are more substantial disagreements between the SC-pseudopotential[21] results and the other calculations, and with the measurements. The exception is for the (222) reflection where the present results are considerably smaller than experiment, while the SC-OPW and SC-pseudopotential results are much closer. Since the calculations of Heaton and Lafon[12] and our own were done in a similar manner except for the choice of exchange-correlation potential and basis functions, the very close agreement between the two sets of results seems to indicate that (at least for Si) the self-consistent charge density is rather insensitive to these choices.

Our structure factor results for Ge also compare very well with the measurements of Matsushita and Kohra[24] and with the SCOPW[29] calculations. Here too our calculated value of F(222) is smaller than the measured value, though closer than was the case for Si. The SCOPW value of F(222) for Ge is almost a factor of two larger than experiment.

GaP, GaAs, ZnS and ZnSe

Figures 4-9 show our calculated valence and deformation maps and bond axis densities for the zinc-blende compounds. Tables III-V compare the absolute values of our calculated structure factors with experiment and with other *ab initio* results, while in Table VI we present our results for both the real and imaginary parts of $F(hkl)$ for all four compounds. It should be noted that the density maps for ZnS and ZnSe include the 3d-states of Zn and Se, since the Zn 3d-states fall in the upper valence band region (see Ref. 1), while for the gallium compounds, the much lower-lying Ga and As 3d-states were kept in the core. Density maps with the Zn and Se 3d-states kept in the core may be found in Ref. 1.

The valence density maps for all four materials in Figs. 4 and 5 show a charge build-up towards the anion sites (P, As, S, or Se). However, the deformation maps and bond axis densities shown in Figs. 6-9 are even more instructive. The deformation maps clearly show that the bonding induced by the crystalline environment is both ionic and covalent. In fact, the deformation maps are qualitatively similar to Si and Ge insofar as they show a bond charge buildup elongated perpendicular to the bond axis, but with the important difference that the deformation bonding charge is shifted towards the anion site. From Figs. 8 and 9 it can be seen that the bond axis deformation charge densities peak towards the anion site, but the bond axis valence densities are shifted even further towards the anion, indicating that a large part of the valence charge asymmetry is due to atomic wave function overlap effects.

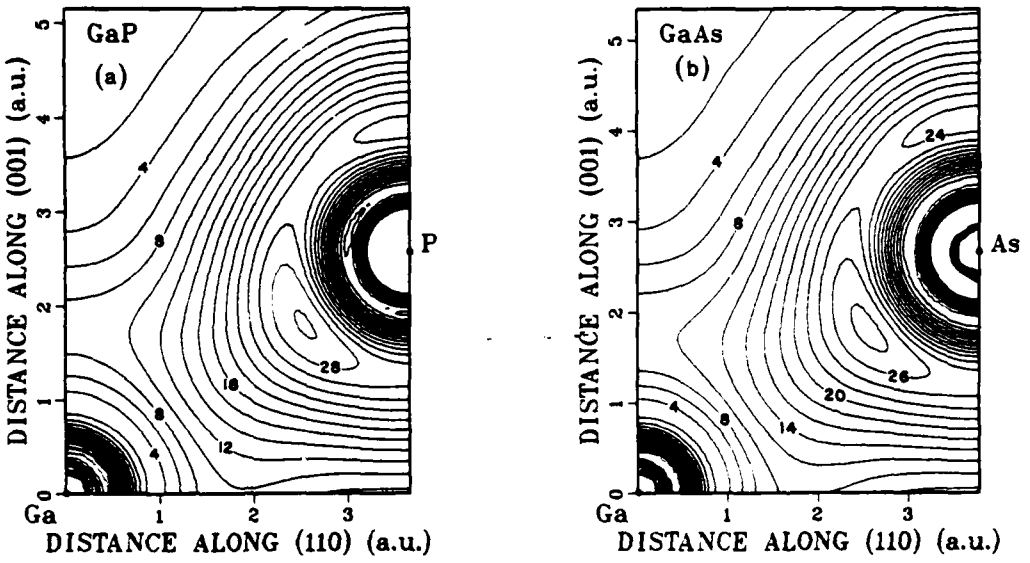

Fig. 4. Calculated self-consistent valence charge density in a portion of the $(1\bar{1}0)$ crystal plane for: a) GaP, and b) GaAs. The contours are in units of electrons/unit cell, and the contour interval is 2 electrons/unit cell.

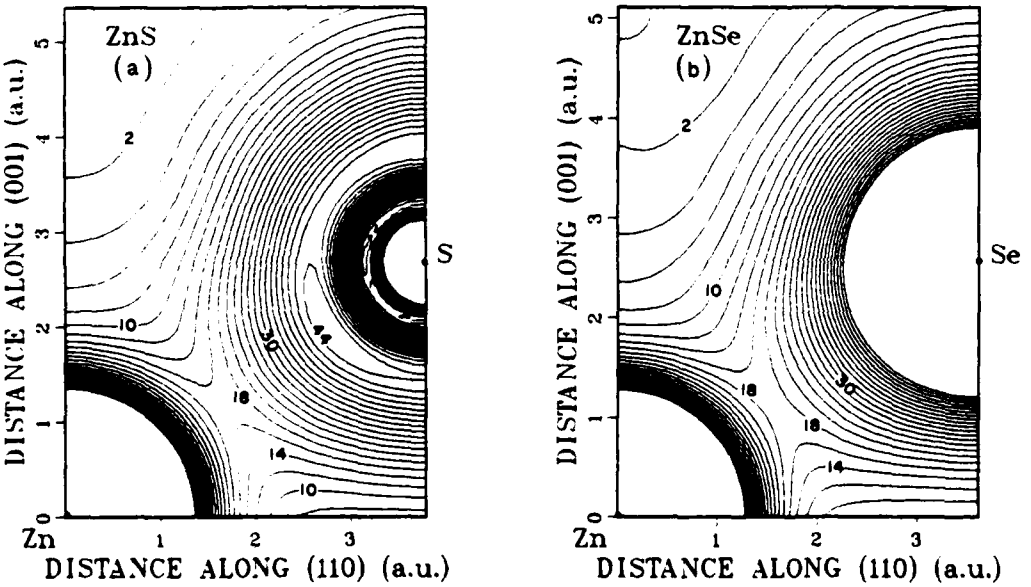

Fig. 5. Calculated self-consistent valence charge density in a portion of the $(1\bar{1}0)$ crystal plane for: a) ZnS, and b) ZnSe. The contours are in units of electrons/unit cell, and the contour interval is 2 electrons/unit cell. For ZnSe we only show contours of 50 or less.

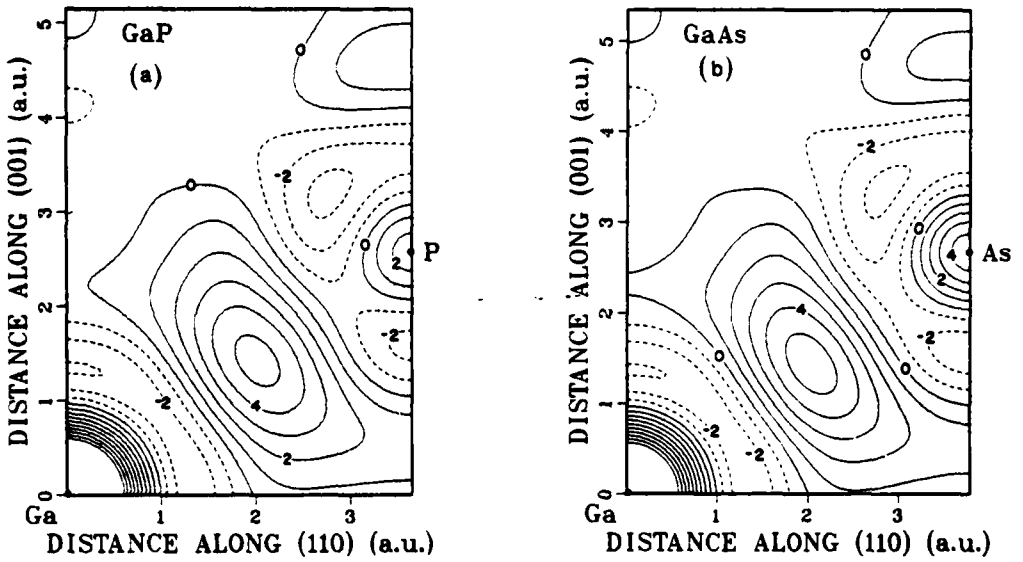

Fig. 6. Calculated valence deformation charge density in a portion of the $(1\bar{1}0)$ crystal plane for: a) GaP, and b) GaAs. The contours are in units of electrons/unit cell, and the contour interval is 1 electron/unit cell.

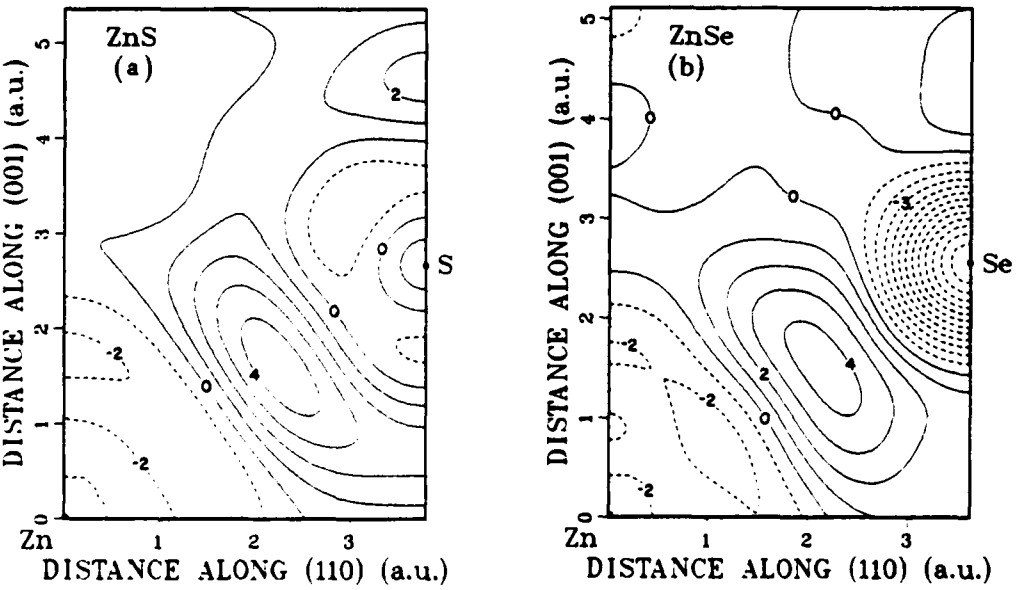

Fig. 7. Calculated valence deformation charge density in a portion of the $(1\bar{1}0)$ crystal plane for: a) ZnS, and b) ZnSe. The contours are in units of electrons/unit cell, and the contour interval is 1 electron/unit cell.

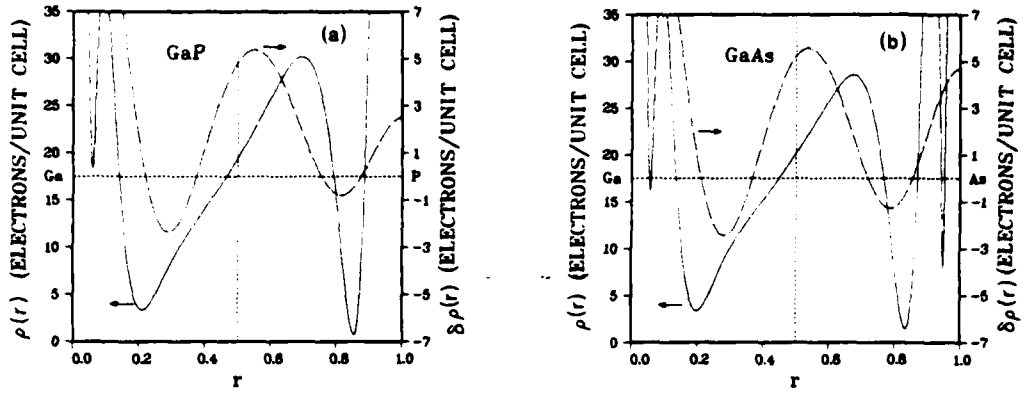

Fig. 8. Calculated $\rho(r)$ (solid lines) and $\delta\rho(r)$ (chain-dotted lines) along the (111) bonding direction for: a) GaP; and b) GaAs. $\rho(r)$ is the self-consistent valence charge density, $\delta\rho(r)$ is the valence deformation charge density (self-consistent minus starting overlapping atomic charge densities), and r is the fraction of the nearest neighbor (bond) distance.

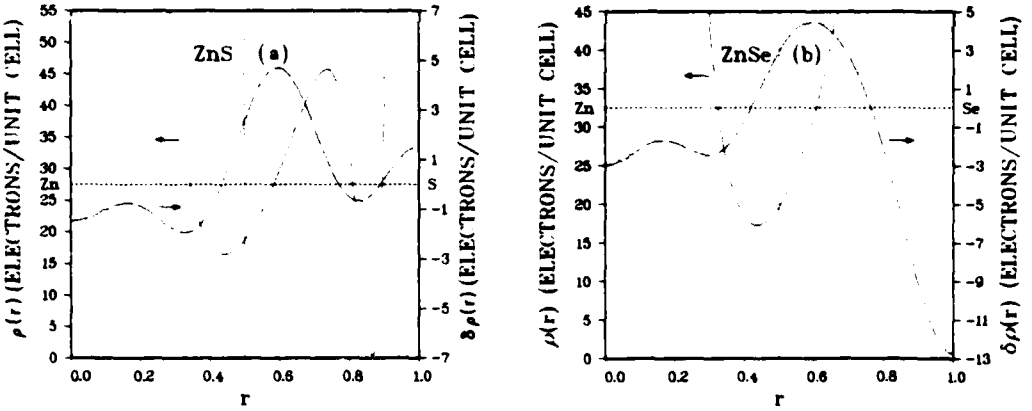

Fig. 9. Calculated $\rho(r)$ (solid lines) and $\delta\rho(r)$ (chain-dotted lines) along the (111) bonding direction for: a) ZnS; and b) ZnSe. $\rho(r)$ is the self-consistent valence charge density, $\delta\rho(r)$ is the valence deformation charge density (self-consistent minus starting overlapping atomic charge densities), and r is the fraction of the nearest neighbor (bond) distance.

Table III. Comparison of Theoretical and Experimental Absolute Values of The X-ray Structure Factors $|F(hkl)|$ for GaAs (in Units of Electrons/Unit Cell)

hkl	Expt.[a]	Expt.[b]	Present Results
000	(64.0)	(64.0)	(64.0)
111	39.44	39.06	38.85
220	47.18	46.66	47.18
311	31.37	31.04	31.25
400	40.84	40.40	40.44
331	27.75	27.45	27.32
422	36.22	35.84	35.80
333	24.37	24.10	24.30
511	24.54	24.27	24.30
440	32.38	32.04	32.15
444	26.94	26.66	26.77

[a]Experimental results of Matsushita and Hayashi (Ref. 31) corrected for anomalous dispersion ($f' = -1.31$) and temperature ($\bar{B} = 0.595$ Å^2).

[b]Experimental results of Matsushita and Hayashi (Ref. 31) corrected for anomalous dispersion ($f' = -1.01$) and temperature ($\bar{B} = 0.629$ Å^2).

Table IV. Comparison of Theoretical and Experimental Absolute Values of The X-ray Structure Factors $|F(hkl)|$ for GaP (in Units of Electrons/Unit Cell)

hkl	Expt.[a]	Present Results
000	(46.0)	(46.0)
111	28.83	28.84
200	14.40	14.63
220	32.19	31.77
311	22.92	22.89
222	12.79	12.45
400	26.19	26.95
331	19.43	19.69
420	10.48	10.44
422	23.86	23.79
333	17.24	17.34
511	17.24	17.35
440	21.01	21.32

[a]Uno and Ishigaki, Ref. 34.

Table V. Comparison of Theoretical and Experimental Absolute Values of the X-ray Structure Factors $|F(hkl)|$ for ZnSe (in Units of Electrons/Unit Cell)

hkl	Experiment[a]	Present	SCOPW[a]
000	(64.0)	(64.0)	(64.0)
111	39.64	38.99	39.06
200	3.72	2.99	2.79
220	47.45	47.16	47.37
311	32.28	31.23	31.38
222	2.91	2.55	2.38
400	40.58	40.27	40.63
331	27.39	27.23	27.59
420	3.02	2.82	2.77
422	35.14	35.63	36.11
440	32.19	32.06	32.55

[a]Ref. 29.

Table VI. Calculated Real and Imaginary Parts of the X-ray Structure Factors $F(hkl)$ for the Zinc-Blende Compounds. The origin is at a cation site, and the units are electrons/unit cell.

hkl	GaAs		GaP		ZnS		ZnSe	
	ReF	ImF	ReF	ImF	ReF	ImF	ReF	ImF
111	26.65	28.27	26.42	11.57	25.62	12.44	25.91	29.13
200	−1.48	0.00	14.63	0.00	13.06	0.00	−2.99	0.00
220	47.18	0.00	31.77	0.00	31.54	0.00	47.16	0.00
311	21.48	−22.70	21.12	−8.83	20.31	−8.86	20.76	−23.33
222	−1.20	0.19	12.45	0.19	11.21	0.10	−2.55	0.13
400	40.44	0.00	26.95	0.00	26.35	0.00	40.27	0.00
331	18.64	19.98	18.20	7.51	17.26	7.77	17.83	20.58
420	−1.39	0.00	10.44	0.00	9.23	0.00	−2.82	0.00
422	35.80	−0.02	23.79	−.03	23.11	−0.04	35.63	−0.04
333	16.40	−17.93	15.92	−6.86	14.98	−7.16	15.57	−18.62
511	16.42	17.91	15.95	6.84	15.00	7.13	15.60	18.59
440	32.15	0.00	21.32	0.00	20.72	0.00	32.06	0.00

In Table III we compare our calculated values of $|F(h\,k\,l)|$ for GaAs with the experimental results of Matsushita and Hayashi[31] corrected for thermal vibrations and anomalous dispersion. The experimental data were determined using the half-width of the Bragg-case diffraction curves measured in the triple crystal arrangement using Cu-Kα radiation (similar to Matsushita and Hayashi's experiments[28] on Ge described above). For the case of polyatomic materials it is considerably more uncertain how to correct for anomalous dispersion (f_j') and determine the Debye-Waller correction (e^{-M}). Different values of f_j' exist in the literature for Ga and As, and the value of B ($M = B(\sin\theta/\lambda)^2$) depends on the choice of f_j'. Matsushita and Hayashi[31] discuss their results in terms of two sets of f_j', from Cromer[32] and from Cromer and Liberman,[33] respectively, without making a clear-cut choice between the sets. We have therefore reduced their experimental data by considering $\overline{f'}$ as the Ga and As mean for both sets: a) $\overline{f'} = -1.31$, $\overline{B} = 0.595\ A^2$, and b) $\overline{f'} = -1.01$, $\overline{B} = 0.629\ A^2$. Both sets of reduced experimental data are shown in Table III and compared with our theoretical results. Given the uncertainty in the $\overline{f'}$ and $\overline{B}$ corrections to the experimental data, and the quoted $\sim$1% accuracy in the measurements, the agreement between theory and experiment is remarkably good.

Uno and Ishigaki[34] have measured the structure factors of GaP using two different methods: a) the angle dispersive method using monochromatized Cu-Kα x-rays and, b) the white x-ray diffraction method, both performed on powder samples. The angle dispersive method results, being more accurate (see Ref. 34), are compared with our calculations in Table IV. The experimental results shown have been corrected to zero temperature using a value of $\overline{B} = 0.84$ obtained from Fig. 3 of Ref. 34 [a $\log(|F_{exp}|/|F_{theory}|)$ plot using Cromer's[32] values for f_{Ga}' and f_P']. As for the GaAs case, there is some uncertainty in the f' and $\overline{B}$ values, and the quoted experimental accuracy is $-$1-3%. Within these experimental uncertainties our results for GaP again agree very well with the measurements.

For ZnSe we compare our results with the experiments and SCOPW calculations of $|F(hkl)|$ of Raccah, *et al.* in Table V. The measurements were done on a powder sample with the thermal and anomalous diffraction corrections taken into account by Raccah, *et al.*[29] (they present the corrected results), with a quoted experimental uncertainty of several percent. Our calculations agree quite well with the measurements, with the most substantial disagreement being for $|F(222)|$. Our results also agree very well with those resulting from the SCOPW calculations.

CONCLUSIONS

We can conclude from the theoretical-experimental comparisons made in this paper that local density theory gives a good description of charge densities in semiconductor systems. The major discrepancy between theory and experiment appears to be that the theory underestimates the charge density asphericity, as evidenced by the too small vlaues of F(222) and bond charge for Si and Ge. This seems to be a general result of many SC calculations for charge and spin densities and is due to the underlying local density approximation. Some examples for metals are shown in Table VII. Improvements in the exchange-correlation functional (e.g., non-local corrections) may resolve these subtle but interesting disagreements between theory and experiment.

Table VII. Directional Anisotropy of Charge and Spin Densities for Transition Metals by Comparing the Ratios of Structure Factors for Wave Vectors of the Same Magnitude.

Element	Structure Factors	Wave Vectors	Theory	Experiment
Ni	Spin	$\frac{(3,3,3)}{(5,1,1)}$	2.179[a]	3.028[b]
Fe	Spin	$\frac{(3,3,0)}{(4,1,1)}$	2.351[c]	2.848[d]
Fe	Charge	$\frac{(3,3,0)}{(4,1,1)}$	1.0025[c]	1.010[e]
				1.011[f]
V	Charge	$\frac{(3,3,0)}{(4,1,1)}$	1.0039[g]	1.024[h]
				1.0085[i]

[a]Ref. 8, [b]Ref. 35, [c]Ref. 9, [d]Ref. 36, [e]Ref. 37, [f]Ref. 38, [g]Ref. 10, [h]Ref. 39, [i]Ref. 40.

However, it is clear from the present study that good quality *ab initio* calculations are capable of giving useful and reliable results for the bonding and chemistry of covalently bonded semiconductors.

ACKNOWLEDGMENTS

The authors are grateful to L. L. Boyer, D. A. Papaconstantopoulos, and W. E. Pickett for comments on the manuscript; and to A. Koppenhaver for technical assistance. This work was supported by the Office of Naval Research, contract no. N00014-79-WR-90028.

REFERENCES

(1) Wang, C.S.,; and Klein, B.M. *Phys. Rev.* **1981**, *B24*, in press.
(2) Wang, C.S.; and Klein, B.M. *Phys. Rev.* **1981**, *B24*, in press.
(3) Lafon, E.E.; Lin, C.C. *Phys. Rev.* **1966**, *152*, 579.
(4) Chaney, R.C.; Tung, T.K.; Lin, C.C.; Lafon, E. *J. Chem. Phys.* **1970**, *52*, 361.
(5) Wang, C.S.; Callaway, J. *Comput. Phys. Commun.* **1978**, *14*, 327.
(6) Ching, W.Y.; Calloway, J. *Phys. Rev.* **1975**, *B11*, 1324; **1974**, *B9*, 5115.
(7) Singhal, S.P.; Callaway, J. *Phys. Rev.* **1977**, *B16*, 1744.
(8) Wang, C.S.; Callaway, J. *Phys. Rev.* **1977**, *B15*, 298; Callaway, J.; Wang, C.S. *Phys. Rev.* **1973**, *B7*, 1096.
(9) Callaway, J.; Wang, C.S. *Phys. Rev.* **1977**, *B16*, 2095; Tawil, R.A.; Callaway, J. *Phys. Rev.* **1973**, *B7*, 4252.
(10) Laurent, D.G.; Wang, C.S.; Callaway, J. *Phys. Rev.* **1978**, *B17*, 455.

(11) Heaton, R.; Lafon, E. *Phys. Rev.* **1978**, *B17*, 1958.
(12) Heaton, R.; Lafon, E. *J. Phys.* **1981**, *C14*, 347.
(13) Simmons, J.E., Lin, C.C.; Fouquet, D.F.; Lafon, E.E.; Chaney, R.C. *J. Phys.* **1975**, *C8*, 1549.
(14) Herman, F.; Skillman, S. "Atomic Structure Calculations," Prentice-Hall: New York, 1963.
(15) Wigner, E. *Phys Rev.* **1934** *46*, 1002.
(16) Euwema, R.N. *Phys. Rev.* **1971**, B4, 4322.
(17) Chaney, R.C.; Norman, F. *Int. J. Quantum Chem.* **1974**, *8*, 465.
(18) Callaway, J.; Fry, J.L. in "Computational Methods in Band Theory"; Marcus, P.M.; Janak, J.F.; Williams, A.R., Ed.; Plenum: New York, 1972; 512.
(19) Chadi, D.J.; Cohen, M.L. *Phys. Rev.* **1973** *B8*, 5747.
(20) Hamann, D.R. *Phys. Rev. Lett.* **1979** , *42*, 662.
(21) Zunger, A.; Cohen, M.L. *Phys. Rev.* **1979**, *B20*, 4082.
(22) Yang, Y.W.; Coppens, P. *Solid State Commun.* **1974**, *15*, 1555.
(23) Scheringer, C. *Acta. Cryst.* **1980**, *A36*, 205.
(24) Matsushita, T.; Kohra, K. *Phys. Stat. Sol.* **1974**, *24*, 531.
(25) DeMarco, J.J.; Weiss, R.J. *Phys. Rev.* **1965**, *137*, A1869.
(26) Yang, Y.W. "Ph.D. Thesis, State Univesity of New York at Buffalo" unpublished, 1976.
(27) Aldred, P.J.E.; Hart, M. *Proc. Roy. Soc. London* **1973**, *A332*, 223.
(28) Roberto, J.B.; Batterman, B.W.; Keating, K.T. *Phys. Rev.* **1974**, *B9*, 2590.
(29) Raccah, P.M.; Euwema, R.N.; Stukel, D.J.; Collins, T.C. *Phys. Rev.* **1970**, *B1*, 756.
(30) Hedin, L.; Lundqvist *J. Phys.* **1971**, *C4*, 2064.
(31) Matsushita, T.; Hayashi, J. *Phys. Stat. Sol.* **1977**, A41, 139.
(32) Cromer, D.T. *Acta. Cryst.* **1965**, *18*, 17.
(33) Cromer, D.T.; Liberman, D. *J. Chem. Phys.* **1970**, *53*, 1891.
(34) Uno, R.; Ishigaki, J. *J. Appl. Cryst.* **1975**, *8*, 578.
(35) Mook, H.A. *Phys. Rev.* **1966**, *148*, 495.
(36) Terasaki, D.; Uchida, Y.; Watanabe, D. *J. Phys. Soc. Jpn.* **1975**, *39*, 1277.
(37) Diana, M.; Mazzone, G. *Phys. Rev.* **1974**, *B9*, 3898.
(38) DeMarco, J.J.; Weiss, R.J. *Phys. Lett.* **1965**, *18*, 92.
(39) Weiss, R.J.; DeMarco, J.J. *Phys. Rev.* **1965**, *140*, A1223.
(40) Diana, M.; Mazzone, G. *Philos. Mag.* **1975**, *32*, 1227.

END

FILMED

2-85

DTIC